Biophysical Journal, Volume *111*

Supplemental Information

Capturing Invisible Motions in the Transition from Ground to Rare Excited States of T4 Lysozyme L99A

Jamie M. Schiffer, Victoria A. Feher, Robert D. Malmstrom, Roxana Sida, and Rommie E. Amaro

Supplementary Figures

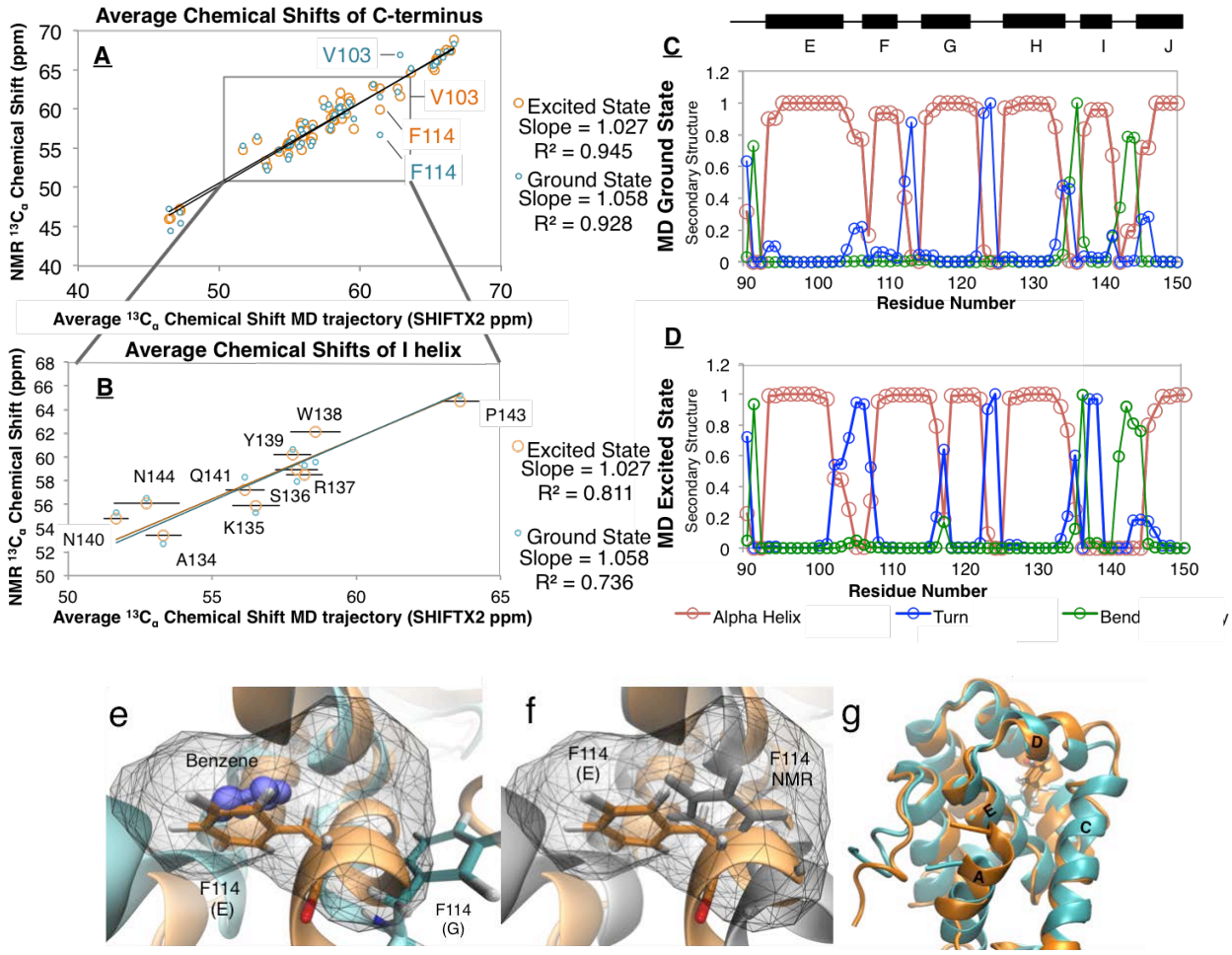

Figure S1 | Characterizing the structures of the T4 lysozyme L99A excited state from MD simulations with SHIFTX2 and secondary structure calculations. (a) The SHIFTX2 average back-calculated chemical shifts of residues in the C-terminal domain (residues 75-155) from the excited state simulated with Anton (x axis) are compared to the chemical shifts determined by relaxation dispersion NMR spectroscopy (y axis) of the excited state (orange). The fits to the experimental ground state chemical shifts are shown for comparison (cyan). (b) Plot that is the same as (a) but looking closer at residues in the I helix. Error bars are showing the standard deviation of the back-calculated chemical shifts of the excited state from the simulation. (c/d) Secondary structures calculated from frames of the ground state and excited states from MD simulation including the alpha helices (red), turns (blue), and bended structures (green). (e) Location of F114 in the buried pocket in the ground (G) and excited (E) states shown in the context of the buried ground state cavity (grey mesh). (f) Same as (e) but showing the location of F114 in the previously published Rosetta model (grey). (g) View of the ground and the excited state structures of the L99A mutant from simulation from the back face of the C-terminal domain to highlight the change in pitch of the A helix in the excited state (orange).

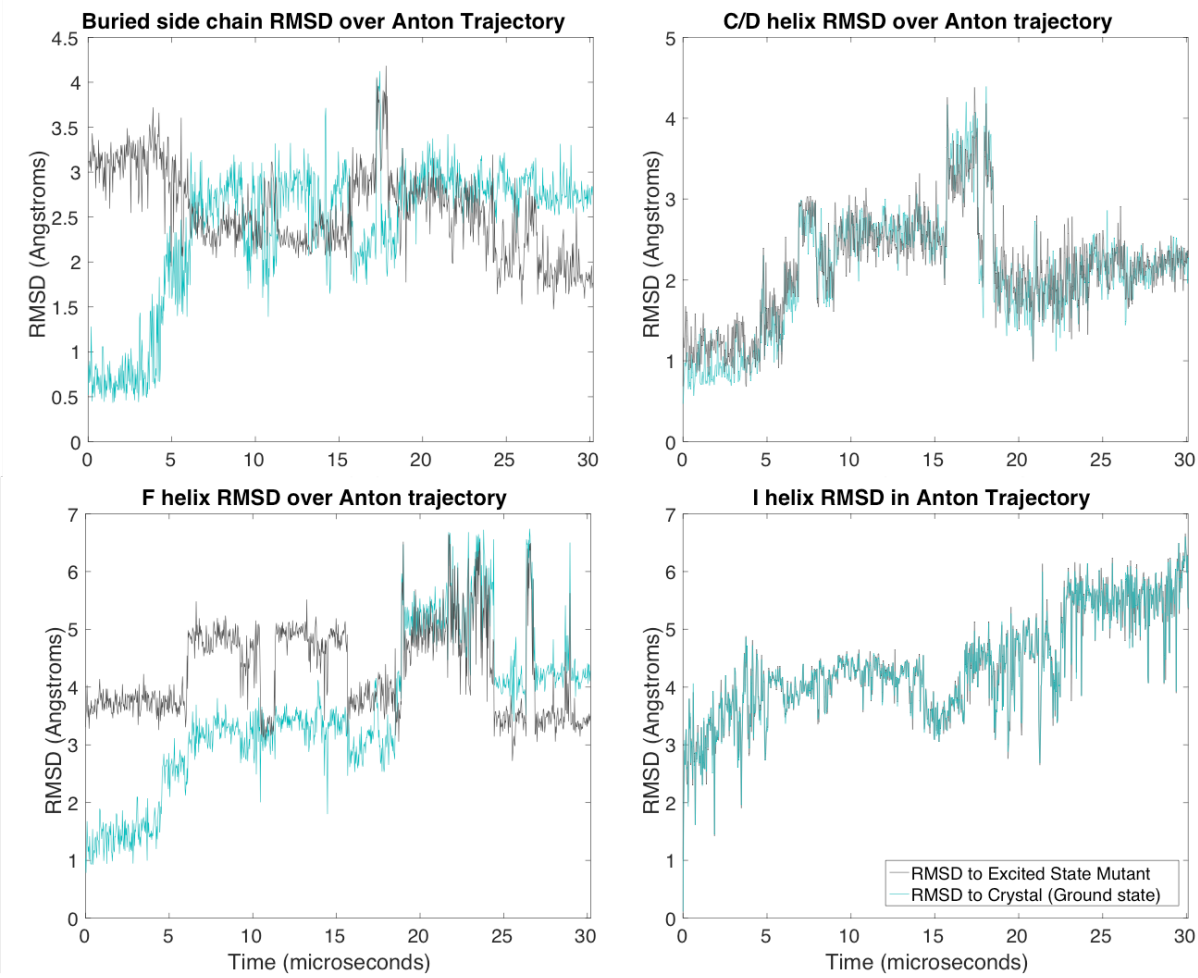

Figure S2 | Root-mean-squared deviation (RMSD) of the backbone atoms in the C-D, F-G, and I helices and in the side chain atoms (residues M102, F114, L133, W138, F153) of the buried hydrophobic residues from the Anton trajectory compared to the excited state mimic mutant and to the ground state crystal structure.

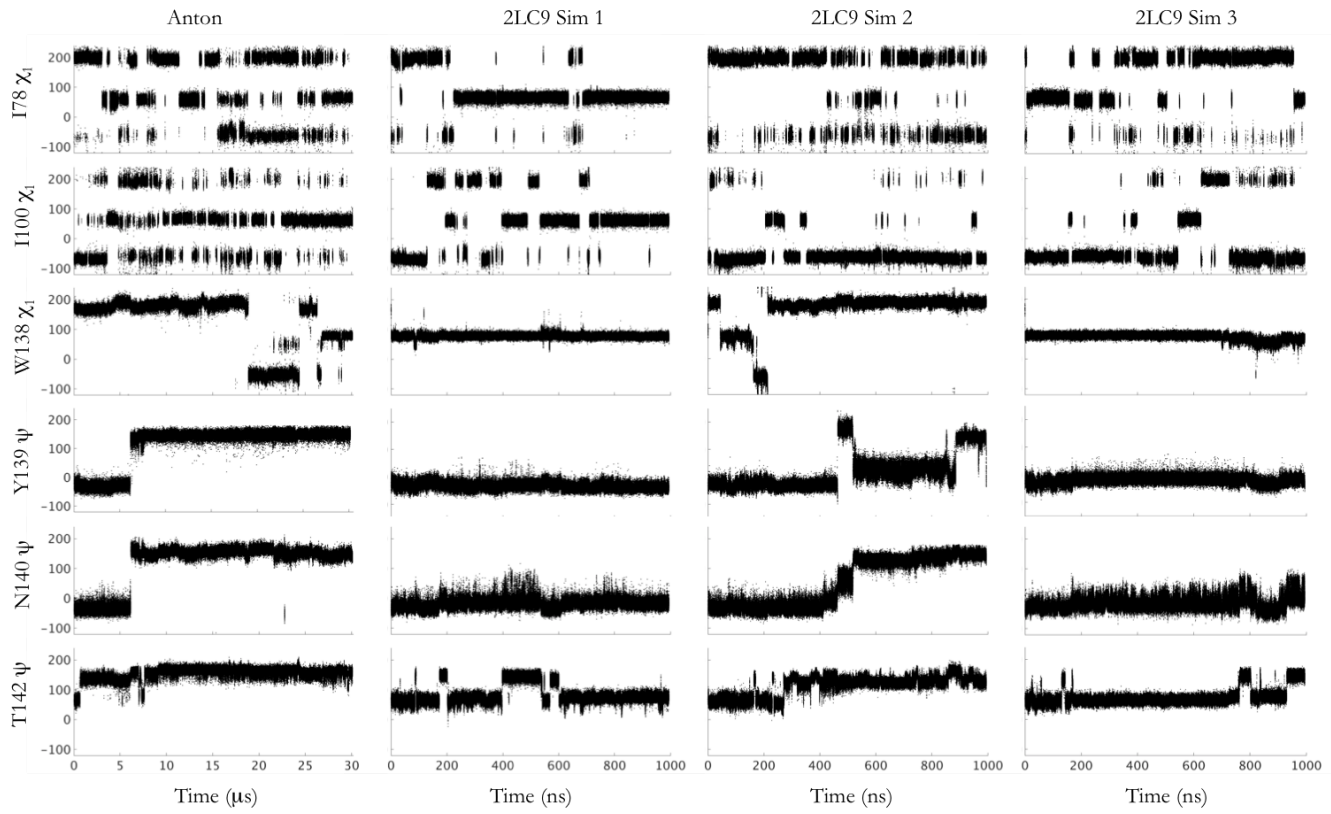

Figure S3 | The χ_1 and ψ angle changes in the Anton trajectory of buried hydrophobic and I helix residues are also witnessed in simulations initiated from the previously published Rosetta model. Residues I100, I78, and W138 all neighbor the buried cavity of the L99A mutant. In the Anton trajectory, these residues sample different χ_1 angles in the transition to the excited state from the ground state, which were not previously seen in the Rosetta model. However, simulations initiated from this Rosetta model also sample these same excited state χ_1 angles in at least one of the triplicate simulations (2LC9_1, 2LC9_2, 2LC9_3). Residues Y139, N140, and T142 also sample unique ψ angles early on in the Anton trajectory. In at least one, if not more, of the triplicate Rosetta model simulations, these same ψ angles are also sampled.

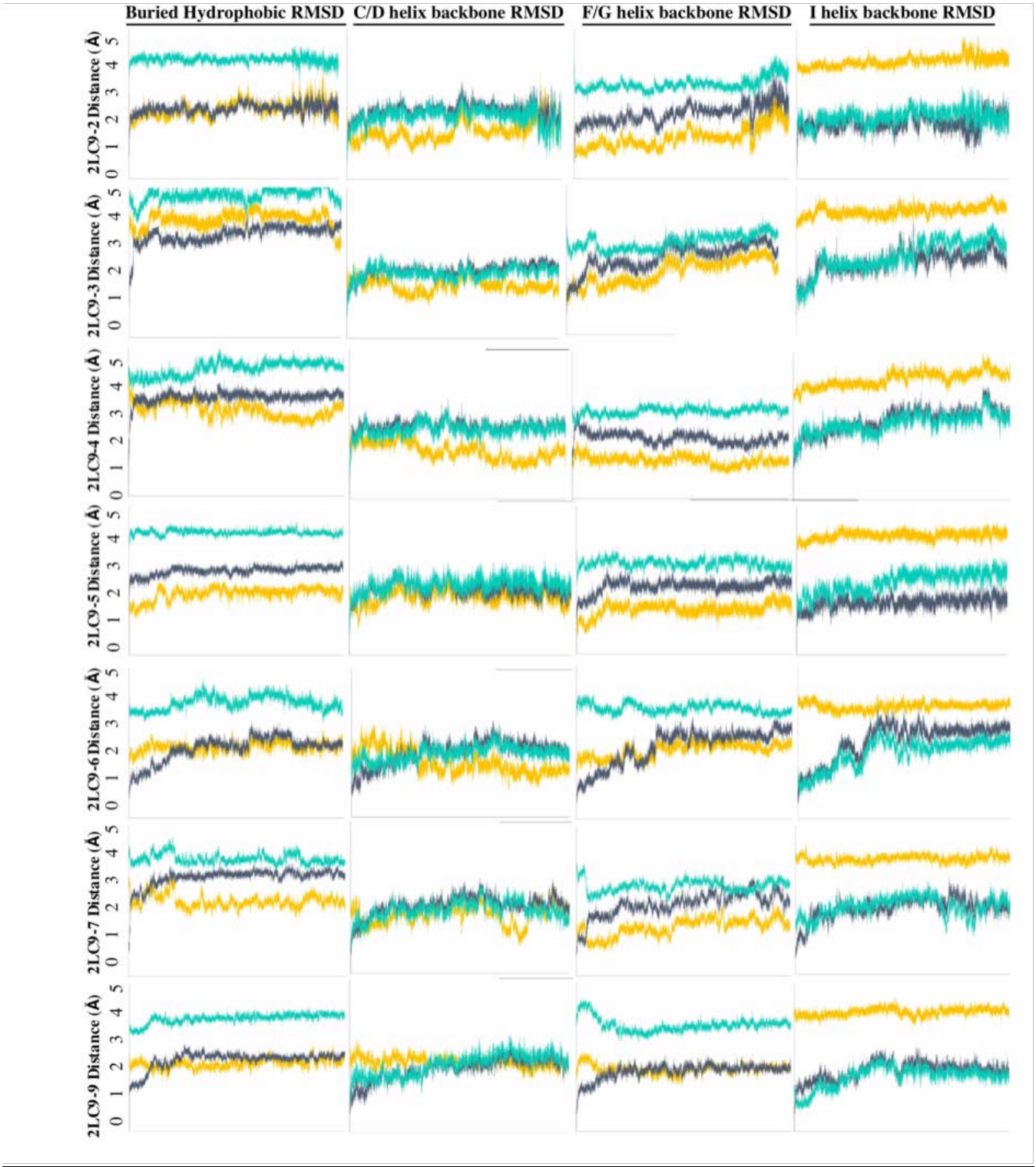

Figure S4 | Average RMSD measurements from simulations of in-silico re-mutated (A113G/P119R) triple mutant model of the L99A excited state (PDB: 2LC9). Each row represents RMSD measurements made during the simulations initiated from a different starting structure, but each were a member of the 2LC9 PDB (10 structures in total). RMSD time plots are showing the RMSD of

the simulated structures to the MD Anton excited state average structure (orange), to the excited state model starting structure (gray, 2LC9), and to the ground state crystal structure of L99A (teal) and are reported as an average over three parallel simulations. The first column is showing the RMSD time plots of buried residues (trace of V78, L87, M102, V103, V111, F114, L133, W138, F153). The second column is showing the RMSD time plots of the backbone of the C/D helix residues (residue 75-90). The third column is showing the RMSD time plots of backbone of the F/G helix residues (residue 108-122). The fourth column is showing the RMSD time plots of the backbone of the I helix residues (residue 135-145).

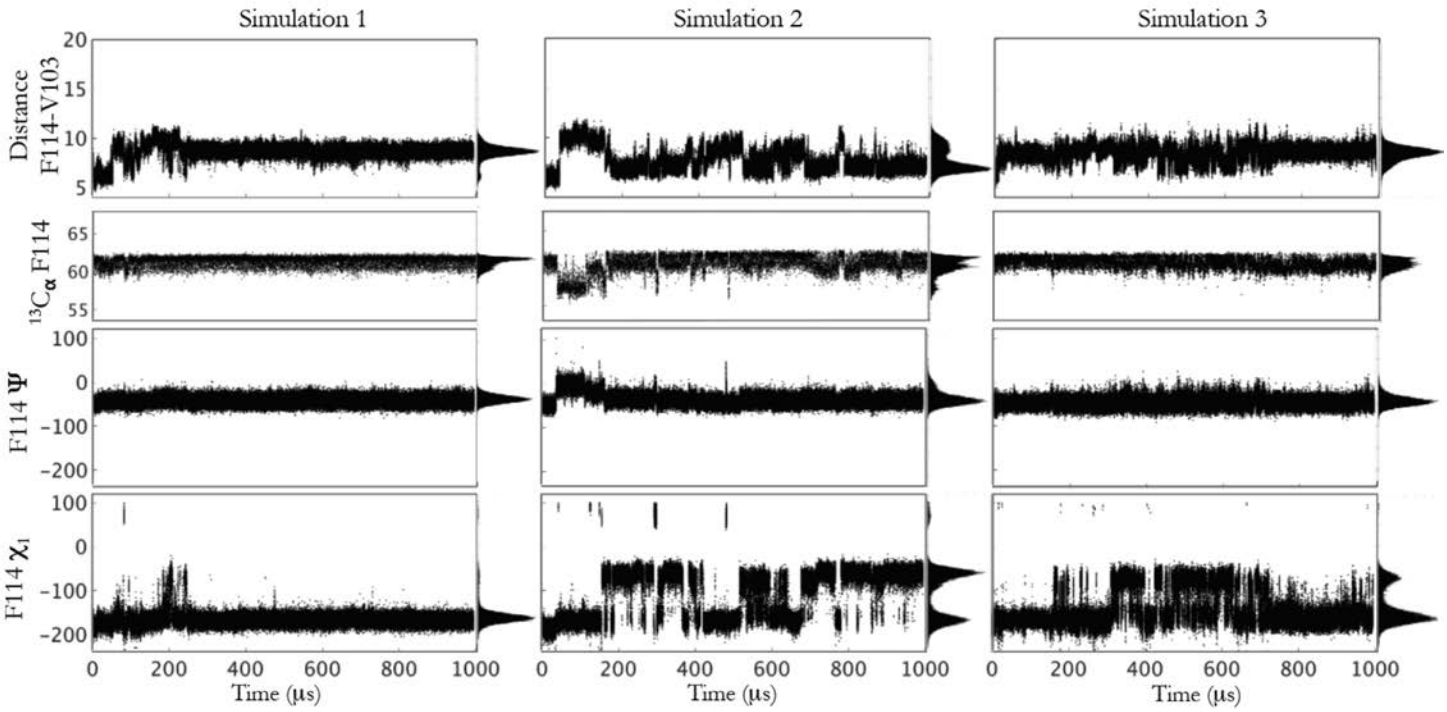

Figure S5 | Analysis of simulations initiated from previous model of the excited state. Distance between F114 phenyl ring and amide nitrogen of V103, back-calculated chemical shift of the $^{13}C_\alpha$ of F114, and ψ and χ_1 angle plots for F114 during the three simulations initiated from the first structure of the previous published NMR excited state model (PDB 2LC9). The population histograms are also shown on the right of each plot.

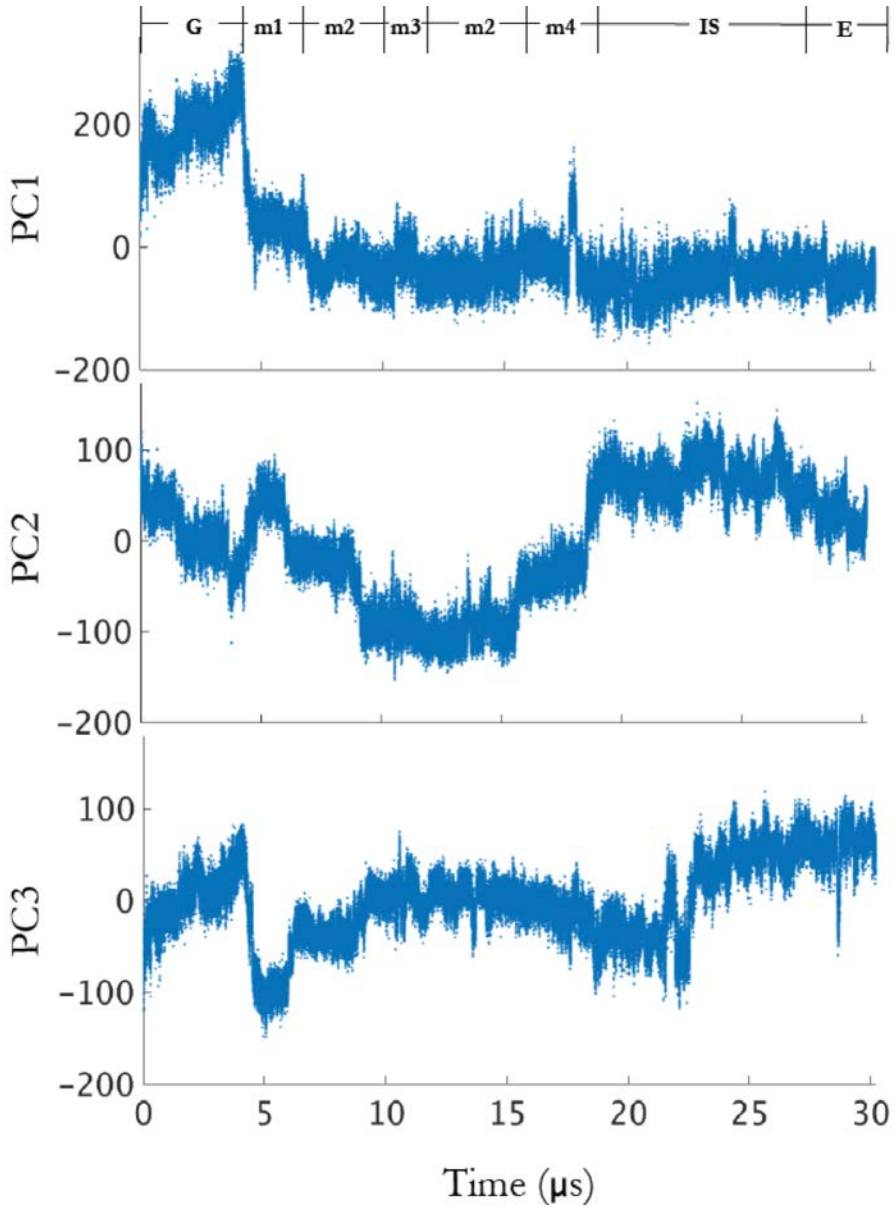

Figure S6 | Principal component (PC) analysis of Anton Trajectory from ground to excited state. Principal component changes over the simulation times for PC1, PC2, and PC3. PC1 identifies all of the metastates and has a slight difference between the IS and E states. PC2 and PC3 identify more clearly the difference between intermediate and excited states. PC1, PC2, and PC3 are accompanied with movies S2-S4 respectively.